JACS
JOURNAL OF THE AMERICAN CHEMICAL SOCIETY

Communication

pubs.acs.org/JACS

Surface-Enhanced Raman Scattering Surface Selection Rules for the Proteomic Liquid Biopsy in Real Samples: Efficient Detection of the Oncoprotein c-MYC

Elena Pazos,[†] Manuel Garcia-Algar,[†,‡] Cristina Penas,[§] Moritz Nazarenus,[‡] Arnau Torruella,[†,‡] Nicolas Pazos-Perez,[‡] Luca Guerrini,[‡] M. Eugenio Vázquez,[§] Eduardo Garcia-Rico,*[,∥] José L. Mascareñas,*[,§] and Ramon A. Alvarez-Puebla*[,†,⊥]

[†]Universitat Rovira i Virgili and Centro de Tecnología Química de Catalunya, Carrer de Marcellí Domingo s/n, 43007 Tarragona, Spain

[‡]Medcom Advance S.A., Av. Roma, 08840 Barcelona, Spain

[§]Centro Singular de Investigación en Química Biolóxica e Materiais Moleculares (CIQUS) and Departamento de Química Orgánica, Universidade de Santiago de Compostela, 15782 Santiago de Compostela, Spain

[∥]Department of Clinical Oncology, Hospital Universitario Hm Madrid-Torrelodones, 28250 Madrid, Spain

[⊥]ICREA, Passeig Lluís Companys 23, 08010 Barcelona, Spain

Supporting Information

ABSTRACT: Blood-based biomarkers (liquid biopsy) offer extremely valuable tools for the noninvasive diagnosis and monitoring of tumors. The protein c-MYC, a transcription factor that has been shown to be deregulated in up to 70% of human cancers, can be used as a robust proteomic signature for cancer. Herein, we developed a rapid, highly specific, and sensitive surface-enhanced Raman scattering (SERS) assay for the quantification of c-MYC in real blood samples. The sensing scheme relies on the use of specifically designed hybrid plasmonic materials and their bioderivatization with a selective peptidic receptor modified with a SERS transducer. Peptide/c-MYC recognition events translate into measurable alterations of the SERS spectra associated with a molecular reorientation of the transducer, in agreement with the surface selection rules. The efficiency of the sensor is demonstrated in cellular lines, healthy donors and a cancer patient.

The molecular characterization of tumors is consistently applied in clinical oncology to guide treatment decisions. These analyses are typically performed on solid tissues acquired through an invasive biopsy at diagnosis. However, tissue biopsies are challenging as they are costly, painful, or potentially risky for the patient. Thus, the development of noninvasive methods to detect and monitor tumors is a major need in oncology. Blood-based biomarkers (liquid biopsy)[1] have a considerable potential for the diagnosis and monitoring of cancer. Circulating tumor cells[2] and circulating tumor nucleic acids[3] are all options, alongside protein markers.[1] However, the protein expression patterns in plasma circulating tumor cells as well as in peripheral blood mononuclear cells fractions remain a largely unexplored aspect.[1]

The protein c-MYC is a helix−loop−helix leucine zipper (bHLHZ) transcription factor encoded by the corresponding *c-myc* gene that plays a major role in coordinating cellular metabolism with cell cycle and has been shown to be elevated or deregulated in up to 70% of human cancers.[4] Unlike other proto-oncogenes whose activity is dependent on mutations, truncations, or gene fusions, the oncogenicity of the *c-myc* gene is usually secondary to loss of transcriptional control leading to over-expression and accumulation of normal protein.[5] Furthermore, the c-MYC protein is not associated with any specific transcriptional program, but it appears to be a universal amplifier of gene expression, increasing the transcription at all active promoters.[6] Thus, the evaluation of the concentration of this protein in blood can be used as a criteria for the diagnosis and monitoring of tumors.

Identification and quantification of proteins in blood is normally performed by using standard immunological techniques such as Western Blot (WB) or ELISA. Although robust, these methods are tedious, lengthy, expensive and, in the case of WB, have low sensitivity. In recent years, surface-enhanced Raman scattering (SERS) spectroscopy[7] has emerged as an excellent alternative for the detection, quantification and characterization of biopolymers. SERS has been employed directly for ultrasensitive quantification of prionic,[8] green[9] or yellow[10] fluorescent proteins, and others.[11] Most of these determinations were carried out in lab solutions because the analysis of protein markers in real samples is extremely challenging due to both the intrinsic complexity of these samples and the usually low concentration (~pg/mL) and poor SERS cross section[12] of the targets. A possible solution relies on the functionalization of the plasmonic materials with chemical species (chemoreceptors) with high SERS cross section and displaying high binding affinity and specificity for the target protein.[12] In this approach, detection is determined by the spectroscopic changes in the chemoreceptor SERS spectrum upon binding with the target.[13] Species such as antibodies, aptamers, or peptides can be used as chemo-

Received: September 1, 2016
Published: October 12, 2016

DOI: 10.1021/jacs.6b08957
J. Am. Chem. Soc. 2016, 138, 14206−14209

receptors.[14] However, these molecules are often characterized by a remarkable small SERS activity, which severely limits their application for direct ultradetection. This issue can be addressed by derivatizing the macromolecular receptor with a terminal moiety with high SERS cross section and affinity for the plasmonic surface to mediate the interaction between the receptor and the metallic substrate.[14a] In this communication, we designed and prepared a SERS-active peptide-conjugate (MB-H1) that binds c-MYC with high affinity and selectivity. Silica microbeads rather homogeneously coated with silver nanoparticles (SiO_2@Ag) were appropriately biofunctionalized with the chemoreceptor (SiO_2@Ag@MB-H1) and successfully used for the quantification of c-MYC protein on laboratory and real samples from healthy donors and a cancer patient.

The chemoreceptor is based on a double mutant peptide (Ser^{520}→Ala, Phe^{522}→Ala) derived from the helix 1 of the helix−loop−helix region of c-MYC (^{515}NELKRAFAALRDQI^{528}, H1), which is known to interact with high affinity and selectivity with c-MYC.[15] To build the SERS probe, we orthogonally attached a 4-mercaptobenzoyl unit (MB) to the side chain amino group of a Lys residue appended at the C-terminus of the H1 peptide. Such modification should not alter the intrinsic helical propensity of the peptide, or its c-MYC-binding properties. The synthesis of the MB-H1 peptide-conjugate is described in the Supporting Information (SI). Citrate-capped silver nanoparticles (AgNPs) of ca. 65 nm diameter (Figure S5A,B) were electrostatically deposited onto 8 μm diameter silica beads (SiO_2@Ag). Previously, the negatively charged silica microparticles were sequentially coated with polyelectrolytes (polyethylenimine, PEI, positive), poly(acrylic acid) (PAA, negative), and again PEI, using the layer-by-layer (LbL) assembly protocol (Figure S5C−E).[16] The UV−vis spectrum of the prepared AgNPs (Figure 1A) shows

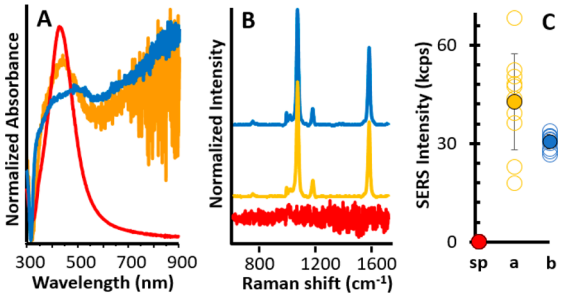

Figure 1. (A) UV−vis spectra of AgNPs in solution (red), aggregated on a glass slide (orange), and anchored on SiO_2 beads (blue). (B) SERS spectra of MB-H1 on nonaggregated (red) and aggregated AgNPs (orange) on glass slides, and on SiO_2@Ag (blue). (C) Corresponding SERS intensities obtained by measuring the peak height of the band at 1075 cm^{-1}.

a defined localized surface plasmon resonance centered at 449 nm. Nanoparticle deposition onto a solid support results in the appearance of an intense and broad feature at longer wavelength, which is an indicator of the interparticle coupling. The SERS fingerprint of MB-H1 on SiO_2@Ag is shown in Figure 1B (blue curve). Remarkably, the SiO_2@Ag offer large surface area, close adsorbent−adsorbate interaction and high density of electromagnetic hot spots, thus combining the benefits of colloids and films, while overcoming important limitations of both. In this regard, we also produced silver-coated glass slides via spin-coating of either nonaggregated (Figure S6B) or aggregated MB-H1-modified AgNPs to compare and evaluate the SERS efficiency of SiO_2@Ag@MB-H1. Results (Figure 1B,C) indicate that no appreciable SERS signal is observed for the nonaggregated AgNPs slides, whereas the aggregated AgNPs layer and SiO_2@Ag display similar SERS intensities but with a smaller standard deviation for the case of beads. The large size of these beads allows their easy localization with a low magnification objective (e.g., ×5) for the later scanning with a higher resolution objective (e.g., ×50 or ×100) (Figure 2A). This paves the way for a drastic reduction of

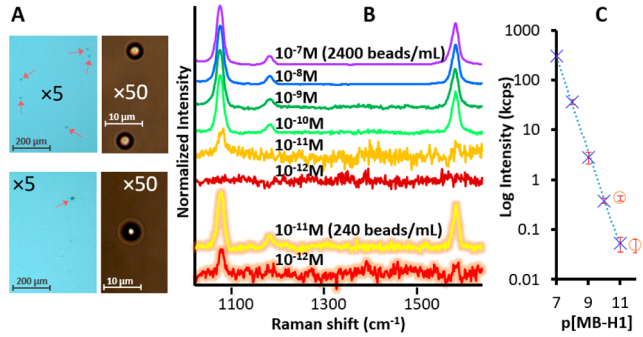

Figure 2. (A) Optical images at low (×5) and high (×50) magnification of beads from a 100 μL aliquot of suspensions with concentrations of 2400 (upper panels) and 240 (bottom panels) beads/mL. (B) SERS spectra of MB-H1 at different concentrations on SiO_2@Ag (2400 beads/mL and, highlighted, 240 beads/mL), and (C) their corresponding intensity at 1075 cm^{-1}.

the amount of plasmonic material required for sensing, which in turn improves the sensitivity by increasing the number of molecules per bead ratio. This is exemplified in Figure 2B,C, which shows that SERS of MB-H1 is distinguishable down to 10 pM for a particle concentration of 2400 beads/mL, whereas lower SiO_2@Ag amounts (240 beads/mL) allow for detection down to 1 pM.

Capturing of the c-MYC target by MB-H1 bound to SiO_2@Ag beads could result in a large set of different perturbations on the SERS spectra of the mercaptobenzoyl moiety, ranging from subtle shifts of the vibrational features to the appearance of new bands. For interpreting such variations, we acquired the Raman and SERS spectra of the SERS-active terminal moiety (4-mercapto-*N*-methylbenzamide, MMB), and those of MB-H1 before and after reaction with c-MYC (Figure 3A). The SERS spectra of MMB and MB-H1 display similar vibrational patterns but with some differences in relative intensities. This result points toward a slight change of the molecular orientation of the mercaptobenzene group on the silver surface when is coupled with a larger molecule such as H1, in full agreement with the surface selection rules.[17] Such perturbation is exacerbated upon binding with the very large c-MYC protein.

To identify the vibrational modes of the mercaptobenzene moiety that are more sensitive to its surface reorientation, we carried out DFT calculations on MMB at the RB3LYP-6311++G(d,p) theory level (Figure 3A).[18] Results indicate that MMB belongs to the C1 point group of symmetry, implying that its structure is not planar. However, because of the strong interaction silver−thiol,[19] we can assume a quasi-perpendicular orientation of the phenyl ring onto the metal.[20] On the other hand, the surface electric field, $\vec{E}$, effectively has only a normal component (Z direction in Figure 3B).[21] Based on these considerations, the intensity of a vibrational mode is proportional to the square of the scalar product of the electric field and the dipole moment derivative of the mode.[22] This scenario defines two degrees of freedom for the phenyl ring to change its orientation upon

DOI: 10.1021/jacs.6b08957
J. Am. Chem. Soc. 2016, 138, 14206−14209

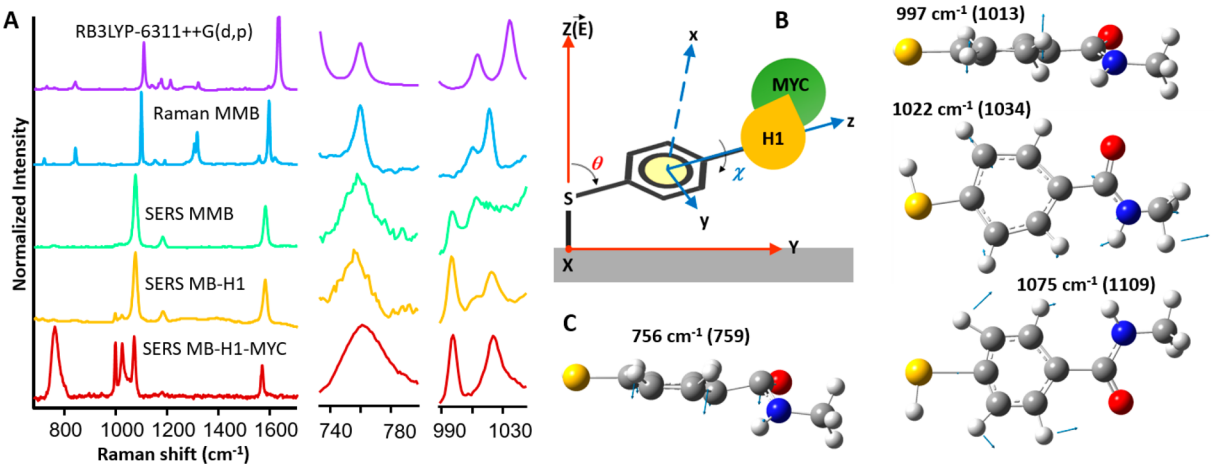

Figure 3. (A) Theoretical and experimental Raman spectrum of MMB and SERS spectra of MMB, MB-H1, and MB-H1 in the presence of c-MYC, on SiO_2@Ag. Magnification of the spectral windows between 730−800 and 990−1050 cm^{-1} are also shown. (B) Model used in the estimation of the molecular orientation. Absolute orientation of the molecule on the surface and relative orientation of the ring over the surface are represented by *XYZ* and *xyz* axes, respectively. (C) Vibrational mode assignment based on DFT calculations (theoretical values are reported into brackets).

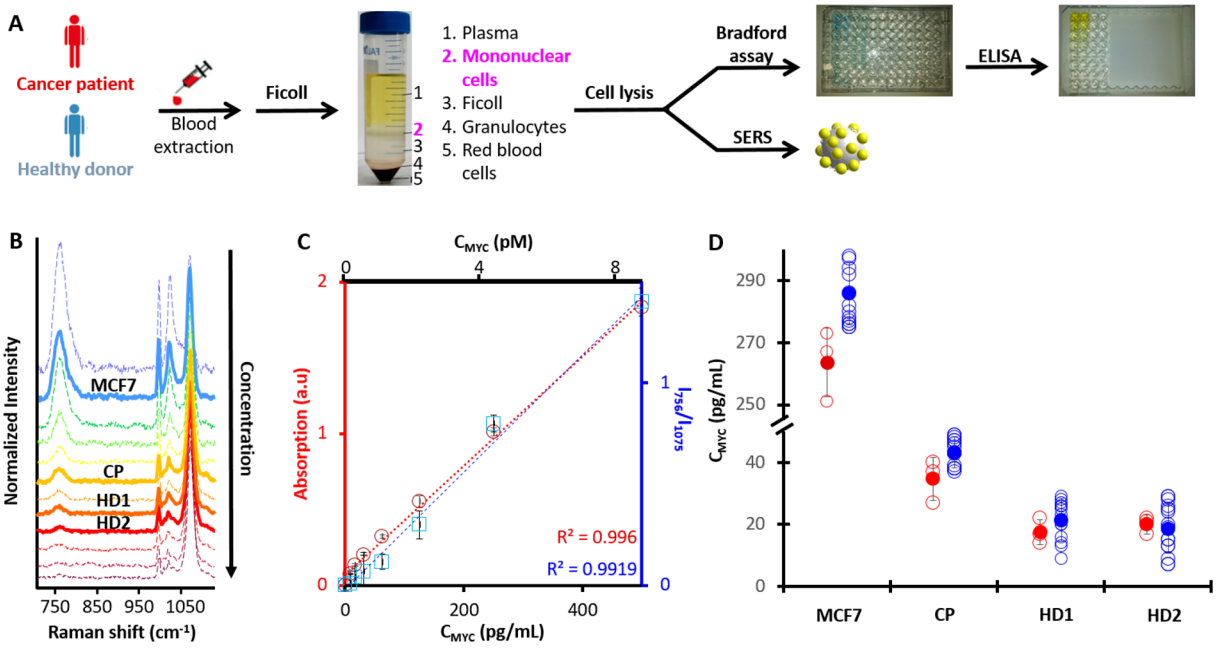

Figure 4. (A) Protocol for the isolation of mononuclear cells in human blood samples from a cancer patient and several healthy donors. (B) SERS spectra of SiO_2@Ag@MB-H1 in the presence of decreasing concentrations of c-MYC (thin dotted lines) and of real samples (thick solid lines). (C) Calibration curves for ELISA (red) and our optical sensor (blue). (D) Results obtained for an epithelial tumor cell line (MCF7), and samples extracted from a cancer patient (CP) and two healthy donors (HD1 and HD2). ELISA in red, and optical sensor in blue. Concentration of c-MYC per million of cells.

interaction with other substances: θ and χ (Figure 3B). θ is the tilt angle of the *z* axis of the mercaptobenzene unit with the surface normal (*Z*). χ is the twist angle of the molecular plane around the *z* axis (which is 0° when *y* is parallel to the surface).

The theoretical Raman MMB spectrum shows good correlation with the experimental observations, which allows the safe assignation of the vibrational modes. The SERS spectrum of MBB displays weak out-of-plane modes, related to the ring plane, at 756 and 997 cm^{-1}, confirming a perpendicular orientation of the phenyl group over the surface. When MMB is included in the MB-H1 structure, we observe a slight intensity increase of these features. More importantly, this effect becomes remarkable when MB-H1 interacts with the oncoprotein due to the c-MYC massive size (57 kDa). In fact, the rise of the out-of-plane bands intensities, up to the same level of the ring breathing at 1075 cm^{-1}, indicates the adoption of a flatter orientation of the ring onto the surface. This is further supported by the drastic intensity increase of the N−C stretching mode (1022 cm^{-1}) upon conjugation with c-MYC. Selection of the spectral markers for c-MYC sensing should take into account that the acquired SERS spectra result from the contributions of both interacting and noninteracting MB-H1 molecules. Thus, rather than monitoring the absolute intensity of a specific feature, c-MYC quantification was performed by recording the ratiometric intensities I_{756}/I_{1075} (ratio between the out-of-plane CCH deformation at 756 cm^{-1} and the in-plane ring breathing at 1075 cm^{-1}).

The efficiency of our sensor was demonstrated with both tumor cell lines and real human samples, whereas ELISA was performed

DOI: 10.1021/jacs.6b08957
J. Am. Chem. Soc. 2016, 138, 14206−14209

to validate the results. The study received ethical approval by the Ethics and Clinical Research Committee of the HM Hospitales Group, and all participants signed a written informed consent form. Figure 4A shows a scheme of the protocol followed for the quantification of c-MYC by ELISA and SERS. Blood samples were obtained from two healthy donors and a patient diagnosed of ovarian adenocarcinoma (stage IV). The patient was in progression at the time of sample collection. The presence of the tumor was confirmed histologically in compliance with common standards. Each sample of peripheral blood (8 mL) was processed in the following 24 h after extraction to obtain the mononuclear cells by a Ficoll process. The mononuclear cells collected from the blood samples as well as those from an epithelial tumor cell line (MCF7) were lysed and centrifuged. Supernatants were then extracted and, for ELISA, the total protein amount was quantified by the Bradford protein assay. Levels of c-MYC were then determined with a total-human c-MYC ELISA kit. In the case of SERS, SiO_2@Ag@MB-H1 (100 μL of a 2400 beads/mL solution, which is equivalent to a concentration of 2.5 $\times 10^6$ molecules of MB-H1 per bead) was directly added to each of the supernatants up to a final concentration of ~218 beads/mL. Then, 100 μL aliquots were cast on glass slides, and beads were analyzed by SERS before the evaporation of the solvent. Figure 4B shows the SERS spectra for both c-MYC standards (in dotted thin lines), the same as used for calibration in ELISA, and the real human samples (in solid thick lines). The corresponding calibrations curves obtained for each method are presented in Figure 4C. Notably, both ELISA and SERS show adequate correlation coefficients with analogous c-MYC detection limits, albeit with a slightly larger standard deviation for the optical method. However, SERS results are obtained within minutes, whereas ELISA assays require lengthy 4−5 h preparation procedures. Similar results are obtained for real samples (Figure 4D). Finally, MCF7 yields to much higher values than real sample, probably because in that case all cells in the culture are cancerous, whereas in the real samples just a small fraction are tumor cells.

In summary, we have developed a rapid, highly specific and sensitive SERS assay for the determination of c-MYC in real blood samples. The sensing scheme relies on the use of specifically designed hybrid materials consisting of silica microparticles coated with interacting silver nanoparticles. The metallic surfaces are bioderivatized with a c-MYC binding peptide modified with a 4-mercaptobenzoyl antenna (MB-H1) that transduces the specific c-MYC recognition events into a measurable alteration of the SERS signal from MB-H1. Deconvolution of the chemoreceptor vibrational fingerprint allowed us to identify characteristic vibrational modes affected by c-MYC complexation. The extent of such spectral changes was quantitatively correlated with the c-MYC content in complex biological media of real samples.

■ ASSOCIATED CONTENT

Supporting Information

The Supporting Information is available free of charge on the ACS Publications website at DOI: 10.1021/jacs.6b08957.

Experimental section; general peptide synthesis procedures; synthesis, characterization and functionalization of SiO_2@Ag beads; cell and human samples preparation; additional SEM/TEM and SERS spectra (PDF)

■ AUTHOR INFORMATION

Corresponding Authors

*R.A.A.-P. ramon.alvarez@urv.cat
*J.L.M. joseluis.mascarenas@usc.es
*E.G.-R. egarcia@hmhospitales.com

Notes

The authors declare no competing financial interest.

■ ACKNOWLEDGMENTS

This work was funded by Marie Curie Actions (FP7/2007-2013, TECNIOspring no. 600388 and PrioSERS FP72014-623527), the European Research Council (Advanced Grant No. 340055), the Spanish MINECO (CTQ2014-59808R, SAF2013-41943-R, CTQ2015-70698-R, CTQ2013-49317-EXP and the orfeo-cinqa network), the Generalitat of Catalonia (2014-SGR-480, AGAUR 2014 052 and AGAUR 2014 054), the Xunta de Galicia (GRC2013-041), and Medcom Advance S.A.

■ REFERENCES

(1) Buder, A.; Tomuta, C.; Filipits, M. *Curr. Opin. Oncol.* **2016**, *28*, 130.
(2) Ignatiadis, M.; Lee, M.; Jeffrey, S. S. *Clin. Cancer Res.* **2015**, *21*, 4786.
(3) Crowley, E.; Di Nicolantonio, F.; Loupakis, F.; Bardelli, A. *Nat. Rev. Clin. Oncol.* **2013**, *10*, 472.
(4) Dang, C. V. *Cell* **2012**, *149*, 22.
(5) Helm, F.; Kammertoens, T.; Lehmann, F. M.; Wilke, A.; Bruns, H.; Mautner, J.; Bornkamm, G. W.; Gerbitz, A. *PLoS One* **2013**, *8*, e77375.
(6) Nie, Z.; Hu, G.; Wei, G.; Cui, K.; Yamane, A.; Resch, W.; Wang, R.; Green, D. R.; Tessarollo, L.; Casellas, R.; Zhao, K.; Levens, D. *Cell* **2012**, *151*, 68.
(7) Schlücker, S. *Angew. Chem., Int. Ed.* **2014**, *53*, 4756.
(8) Alvarez-Puebla, R. A.; Agarwal, A.; Manna, P.; Khanal, B. P.; Aldeanueva-Potel, P.; Carbó-Argibay, E.; Pazos-Pérez, N.; Vigderman, L.; Zubarev, E. R.; Kotov, N. A.; Liz-Marzán, L. M. *Proc. Natl. Acad. Sci. U. S. A.* **2011**, *108*, 8157.
(9) Habuchi, S.; Cotlet, M.; Gronheid, R.; Dirix, G.; Michiels, J.; Vanderleyden, J.; De Schryver, F. C.; Hofkens, J. *J. Am. Chem. Soc.* **2003**, *125*, 8446.
(10) Singhal, K.; Kalkan, A. K. *J. Am. Chem. Soc.* **2010**, *132*, 429.
(11) (a) Lin, L.; Tian, X.; Hong, S.; Dai, P.; You, Q.; Wang, R.; Feng, L.; Xie, C.; Tian, Z.-Q.; Chen, X. *Angew. Chem., Int. Ed.* **2013**, *52*, 7266. (b) Feng, M.; Tachikawa, H. *J. Am. Chem. Soc.* **2008**, *130*, 7443.
(12) Alvarez-Puebla, R. A.; Liz-Marzan, L. M. *Chem. Soc. Rev.* **2012**, *41*, 43.
(13) Guerrini, L.; Arenal, R.; Mannini, B.; Chiti, F.; Pini, R.; Matteini, P.; Alvarez-Puebla, R. A. *ACS Appl. Mater. Interfaces* **2015**, *7*, 9420.
(14) (a) Guerrini, L.; Pazos, E.; Penas, C.; Vázquez, M. E.; Mascareñas, J. L.; Alvarez-Puebla, R. A. *J. Am. Chem. Soc.* **2013**, *135*, 10314. (b) Liu, S.; Zhang, X.; Luo, W.; Wang, Z.; Guo, X.; Steigerwald, M. L.; Fang, X. *Angew. Chem., Int. Ed.* **2011**, *50*, 2496. (c) Wang, Y.; Lee, K.; Irudayaraj, J. *Chem. Commun.* **2010**, *46*, 613.
(15) (a) Draeger, L. J.; Mullen, G. P. *J. Biol. Chem.* **1994**, *269*, 1785. (b) Bidwell, G. L.; Raucher, D. *Mol. Cancer Ther.* **2005**, *4*, 1076.
(16) Decher, G. *Science* **1997**, *277*, 1232.
(17) (a) Moskovits, M.; Suh, J. S. *J. Phys. Chem.* **1984**, *88*, 5526. (b) Moskovits, M.; Suh, J. S. *J. Phys. Chem.* **1988**, *92*, 6327.
(18) Frisch et al. *Gaussian 09*, Rev. B01; Gaussian, Inc.:Wallingford CT, 2009.
(19) Sellers, H.; Ulman, A.; Shnidman, Y.; Eilers, J. E. *J. Am. Chem. Soc.* **1993**, *115*, 9389.
(20) Chang, S.-C.; Chao, I.; Tao, Y.-T. *J. Am. Chem. Soc.* **1994**, *116*, 6792.
(21) Ataka, K.-i.; Yotsuyanagi, T.; Osawa, M. *J. Phys. Chem.* **1996**, *100*, 10664.
(22) Allara, D. L.; Nuzzo, R. G. *Langmuir* **1985**, *1*, 52.

DOI: 10.1021/jacs.6b08957
J. Am. Chem. Soc. 2016, 138, 14206−14209